JOURNAL OF THERMOPHYSICS AND HEAT TRANSFER
Vol. 18, No. 3, July–September 2004

Fluid Flow and Heat Transfer from a Cylinder Between Parallel Planes

W. A. Khan,* J. R. Culham,† and M. M. Yovanovich‡
University of Waterloo, Waterloo, Ontario N2L 3G1, Canada

An integral approach is employed to investigate the effects of blockage on fluid flow and heat transfer from a circular cylinder confined between parallel planes. The integral form of the boundary-layer momentum equation is solved using the modified von Kármán–Pohlhausen method, which uses a fourth-order velocity profile inside the hydrodynamic boundary layer. The potential flow velocity, outside the boundary layer, is obtained by the method of images. A third-order temperature profile is used in the thermal boundary layer to solve the energy integral equation for isothermal and isoflux boundary conditions. Closed-form solutions are obtained for the fluid flow and heat transfer from the cylinder with blockage ratio and Reynolds and Prandtl numbers as parameters. It is shown that the blockage ratio controls the fluid flow and the transfer of heat from the cylinder and delays the separation. The results for both thermal boundary conditions are found to be in a good agreement with experimental/numerical data for a single circular cylinder in a channel.

Nomenclature

b	=	blockage ratio, identical to D/S_T
C_D	=	total drag coefficient
C_{Df}	=	friction drag coefficient
C_{Dp}	=	pressure drag coefficient
C_f	=	skin-friction coefficient
C_p	=	pressure coefficient
c_p	=	specific heat of fluid, J/kg · K
D	=	cylinder diameter, m
D_f	=	shear force in flow direction, N
D_p	=	pressure force in flow direction, N
$\bar{h}$	=	average heat transfer coefficient, W/m^2 · K
j	=	number of cylinders in transverse direction
k	=	thermal conductivity, W/m · K
Nu_D	=	average Nusselt number based on diameter of cylinder, identical to $\bar{h}\,D/k_f$
Pr	=	Prandtl number, identical to ν/α
p	=	pressure, N/m^2
q	=	heat flux, W/m^2
Re_D	=	Reynolds number, identical to DU_∞/ν
r, θ	=	polar coordinates
S_T	=	vertical distance between parallel planes
s	=	distance along curved surface of circular cylinder measured from forward stagnation point, m
T	=	temperature, °C
$U(s)$	=	potential flow velocity just outside boundary layer, m/s
u, v	=	velocity components in boundary layer, m/s
$w(z)$	=	complex potential in Cartesian coordinates, m^2/s
x, y	=	Cartesian coordinates
Y	=	distance normal to and measured from surface of circular cylinder, m
z	=	complex variable in Cartesian coordinates, m
α	=	thermal diffusivity, m^2/s
δ	=	hydrodynamic boundary-layer thickness, m
δ_T	=	thermal boundary-layer thickness, m
δ_1	=	displacement thickness, m
δ_2	=	momentum thickness, m
ζ	=	dummy variable
η	=	dimensionless normal distance
θ	=	angle measured, rad or deg
λ	=	pressure gradient parameter
μ	=	absolute viscosity of fluid, kg/m · s
ν	=	kinematic viscosity of fluid, m^2/s
ρ	=	density of the fluid, kg/m^3
τ	=	shear stress, N/m^2
ψ, ϕ	=	stream and potential functions, m^2/s

Subscripts

f	=	fluid or friction
p	=	pressure
r, θ	=	plane polar coordinates
s	=	separation
T	=	temperature
w	=	wall
∞	=	freestream conditions

Introduction

THE main objective of this study is to investigate analytically the effects of blockage ratio $b = D/S_T$ on the fluid flow and heat transfer from a cylinder under different thermal boundary conditions. This parameter plays an important role in determining the fluid flow and heat transfer from a cylinder confined between parallel planes. In practice, a cylinder is placed in flows restricted by walls. This configuration is found in many applications, such as crossflow heat exchangers, shrouded heat sinks, and electric heating elements in boilers. It has been observed by Žukauskas[1] and others that, as the blockage ratio increases, the velocity around the circular cylinder outside the boundary layer increases and the pressure and velocity distributions inside the boundary layer are changed accordingly. Potential flow velocity outside the boundary layer can be obtained by the method of images, which is a technique used in potential flow modeling to represent the presence of a channel wall by creating an image of the cylinder.

The fluid flow and heat transfer from a cylinder (infinite flow conditions) have been studied analytically by Khan et al.,[2] and experimentally/numerically by many researchers including Žukauskas,[1] Roshko,[3] Achenbach,[4] Schlichting,[5] Wieselsberger,[6] Churchill,[7] Sucker and Brauer,[8] Žukauskas and Žiugžda,[9] Eckert

Received 31 October 2003; presented as Paper 2004-493 at the 42nd Aerospace Sciences Meeting and Exhibit, Reno, NV, 5–8 January 2004; revision received 30 January 2004; accepted for publication 31 January 2004.

*Graduate Research Assistant, Department of Mechanical Engineering, Microelectronics Heat Transfer Laboratory.
†Director, Microelectronics Heat Transfer Laboratory.
‡Distinguished Professor Emeritus, Department of Mechanical Engineering, Microelectronics Heat Transfer Laboratory. Fellow AIAA.

and Soehngen,[10] Churchill and Bernstein,[11] Morgan,[12] Hilpert,[13] Refai Ahmed and Yovanovich,[14] Krall and Eckert,[15] Giedt,[16] and Sarma and Sukhatme.[17] However, the problem of fluid flow and heat transfer from a cylinder placed inside a channel has not been studied analytically so far.

A review of existing literature reveals that few experimental/numerical studies exist regarding the configuration of the present problem. Perkins and Leppert[18] investigated local heat transfer coefficients from a uniformly heated cylinder with water in crossflow. They used both potential flow and experimental pressure distributions to investigate and correlate the effects of blockage on the velocity and heat transfer distributions.

Žukauskas[1] analyzed the work of Akilba'yev et al.[19] about the influence of channel blockage on the flow and heat transfer of a tube in a restricted channel. According to Žukauskas,[1] they showed that increasing channel blockage ratio from 0 to 0.8 caused the minimum pressure point to be displaced from $\theta = 70$ to 90 deg, and the separation point to move downstream to $\theta = 100$ deg. Their theoretical calculations, by the method of Merk[20] using the potential flow velocity distribution, showed that the heat transfer on the front portion of the tube increases with an increase in blockage ratio. Žukauskas and Žiugžda[9] performed a series of experiments with different freestream geometries to investigate the effects of channel blockage. They expressed the velocity distribution in the outer boundary layer in terms of channel blockage and used it to estimate the heat transfer behavior of a cylinder. Vaitiekünas et al.[21] investigated numerically the effects of the channel blockage on the dimensionless shear stress, the location of $U_{\max}$, point of boundary-layer detachment, and the local heat transfer coefficients. They approximated the velocity distribution outside the boundary layer by the modified Hiemenz polynomial in which the coefficients are functions of channel blockage. These functions were based on the analysis of the experimental data of Žukauskas and Žiugžda.[9] They[21] found satisfactory agreement with the experimental results of Žukauskas and Žiugžda.

Hattori and Takahashi[22] performed experiments on forced convection heat transfer from a single row of circular cylinders in crossflow. They measured local and average Nusselt numbers for a cylinder in the Reynolds number range from 80 to 6×10^3 and gave a correlation for the average Nusselt number. Later Yamamoto and Hattori[23] verified numerically their heat transfer values for the same arrangement. They found good agreement with those obtained from experiments in water by Hattori and Takahashi.[22]

It is obvious from the literature survey that no analytical study exists to give a closed-form solution for the fluid flow and heat transfer from a circular cylinder in a channel for a wide range of blockage ratios, Reynolds numbers, and Prandtl numbers. In this study, a circular cylinder in a channel is considered in crossflow with a Newtonian fluid ($Pr \geq 0.71$) to investigate the effects of the blockage ratio on the fluid flow and heat transfer from the cylinder for a wide range of parameters, including blockage ratio, Reynolds numbers, and Prandtl numbers. Closed-form solutions are obtained for the drag coefficients and Nusselt numbers under different thermal boundary conditions, which can be used for a wide range of parameters.

Analysis

Consider a uniform flow of a Newtonian fluid ($Pr \geq 0.71$) past a fixed circular cylinder of diameter D, confined between parallel planes, as shown in Fig. 1. The approaching velocity of the fluid is U_∞ and the ambient temperature is assumed to be T_∞. The surface temperature of the cylinder wall is T_w in the case of the isothermal cylinder and the heat flux is q for the isoflux boundary condition. The flow is assumed to be laminar, steady, and two dimensional.

Using an order-of-magnitude analysis, the reduced equations of continuity, momentum, and energy in the plane polar coordinates for an incompressible fluid can be written as follows:

the continuity,

$$\frac{\partial u_r}{\partial r} + \frac{u_r}{r} + \frac{1}{r}\frac{\partial u_\theta}{\partial \theta} = 0 \tag{1}$$

the θ momentum,

$$u_r \frac{\partial u_\theta}{\partial r} + \frac{u_\theta}{r}\frac{\partial u_\theta}{\partial \theta} = -\frac{1}{r\rho}\frac{\partial p}{\partial \theta} + \nu\left(\frac{\partial^2 u_\theta}{\partial r^2} + \frac{1}{r}\frac{\partial u_\theta}{\partial r} - \frac{u_\theta}{r^2}\right) \tag{2}$$

the r momentum,

$$\frac{\partial p}{\partial r} = 0 \tag{3}$$

the energy,

$$u_r \frac{\partial T}{\partial r} + \frac{u_\theta}{r}\frac{\partial T}{\partial \theta} = \alpha\left(\frac{\partial^2 T}{\partial r^2} + \frac{1}{r}\frac{\partial T}{\partial r}\right) \tag{4}$$

These equations can be rewritten by adopting a curvilinear system of coordinates in which s denotes distance along the curved surface of the circular cylinder measured from the forward stagnation point A and Y is the distance normal to and measured from the surface as shown in Fig. 2. In this system of coordinates, the velocity components u_θ and u_r are replaced by u and v in the local s and Y directions, whereas $r\,\mathrm{d}\theta$ and $\mathrm{d}r$ are replaced by $\mathrm{d}s$ and $\mathrm{d}Y$, respectively. The potential flow velocity just outside the boundary layer is denoted by $U(s)$, which will be determined by the method of images. Therefore, the governing equations in this curvilinear system will be as follows:

the continuity,

$$\frac{\partial u}{\partial s} + \frac{\partial v}{\partial Y} = 0 \tag{5}$$

the s momentum,

$$u\frac{\partial u}{\partial s} + v\frac{\partial u}{\partial Y} = -\frac{1}{\rho}\frac{\mathrm{d}p}{\mathrm{d}s} + \nu\frac{\partial^2 u}{\partial Y^2} \tag{6}$$

the Y momentum,

$$\frac{\mathrm{d}p}{\mathrm{d}Y} = 0 \tag{7}$$

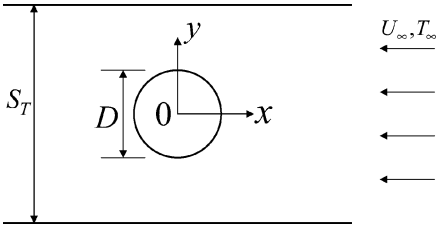

Fig. 1 Physical model and coordinate system.

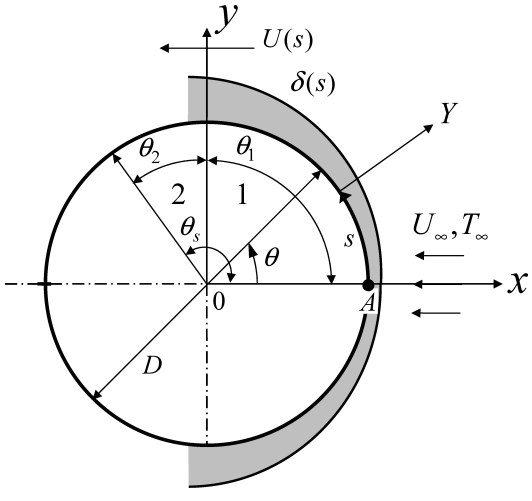

Fig. 2 Flow over a circular cylinder.

the energy,

$$u\frac{\partial T}{\partial s}+v\frac{\partial T}{\partial Y}=\alpha\frac{\partial^2 T}{\partial Y^2} \tag{8}$$

the Bernoulli equation,

$$-\frac{1}{\rho}\frac{\mathrm{d}p}{\mathrm{d}s}=U(s)\frac{\mathrm{d}U(s)}{\mathrm{d}s} \tag{9}$$

Hydrodynamic Boundary Conditions

At the cylinder surface, that is, at $Y=0$,

$$u=0, \qquad \frac{\partial^2 u}{\partial Y^2}=\frac{1}{\mu}\frac{\partial p}{\partial s} \tag{10}$$

At the edge of the boundary layer, that is, at $Y=\delta(s)$,

$$u=U(s), \qquad \frac{\partial u}{\partial Y}=0, \qquad \frac{\partial^2 u}{\partial Y^2}=0 \tag{11}$$

Thermal Boundary Conditions

The boundary conditions for the uniform wall temperature (UWT) and uniform wall flux (UWF) are

$$Y=0,\begin{cases} T=T_w & \text{for UWT} \\ \dfrac{\partial T}{\partial Y}=-\dfrac{q}{k_f} & \text{for UWF} \end{cases} \tag{12}$$

$$Y=0, \qquad \frac{\partial^2 T}{\partial Y^2}=0 \tag{13}$$

$$Y=\delta_T, \qquad T=T_\infty, \qquad \frac{\partial T}{\partial Y}=0 \tag{14}$$

Velocity Distribution Inside Boundary Layer

Assuming a thin boundary layer around the cylinder, the velocity distribution in the boundary layer can be approximated by a fourth-order polynomial as suggested by Pohlhausen,[24]

$$u/U(s)=(2\eta-2\eta^3+\eta^4)+(\lambda/6)(\eta-3\eta^2+3\eta^3-\eta^4) \tag{15}$$

where $0\le\eta=Y/\delta(s)\le 1$ and λ is the pressure gradient parameter given by

$$\lambda=\frac{\delta^2}{\nu}\frac{\mathrm{d}U(s)}{\mathrm{d}s} \tag{16}$$

With the help of velocity profiles, Schlichting[5] showed that the parameter λ is restricted to the range $-12\le\lambda\le 12$.

Velocity Distribution Outside Boundary Layer

When the method of images is used, a cylinder confined between parallel planes (Fig. 1) can be modeled as a system of infinite transverse row of doublets superimposed on a uniform flowfield (Fig. 3). Kochin et al.[25] and Perkins and Leppert[18] pointed out this case. For this case, the complex potential can be written as

$$\begin{aligned} w(z) &= U_\infty z+\sum_{j=-\infty}^{\infty}\frac{\mu}{2\pi(z-ijS_T)} \\ &= U_\infty z+\frac{\mu}{2S_T}\coth\left(\frac{\pi z}{S_T}\right) \end{aligned} \tag{17}$$

where j is the number of doublets or cylinders. Therefore, the complex velocity will be

$$w'(z)=U_\infty-\left(\mu\pi/2S_T^2\right)\left[1/\sinh^2(\pi z/S_T)\right] \tag{18}$$

At the stagnation points, $z=\pm D/2$ and $w'(\pm D/2)=0$. Therefore, Eq. (18) gives

$$\mu/2S_T=(U_\infty S_T/\pi)\sinh^2(\pi D/2S_T) \tag{19}$$

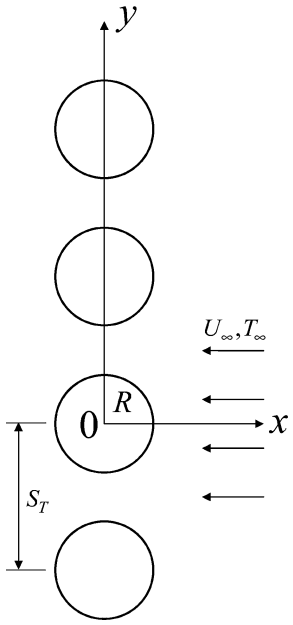

Fig. 3 Transverse row of doublets or circular cylinders.

When this value is substituted into Eq. (17), the required complex potential will be

$$w(z)=\phi+i\psi=U_\infty[z+C\coth(\pi z/S_T)] \tag{20}$$

where ϕ and ψ are the potential and stream functions and C is a constant given by

$$C=(S_T/\pi)\sinh^2(\pi D/2S_T) \tag{21}$$

The stream function ψ in polar coordinates (r,θ) can be obtained from Eq. (20) as follows:

$$\psi=U_\infty r\sin\theta - C\left[U_\infty\frac{\sin(2\pi r\sin\theta/S_T)}{\cosh(2\pi r\cos\theta/S_T)-\cos(2\pi r\sin\theta/S_T)}\right] \tag{22}$$

The radial and transverse components of velocity at the surface of the cylinder can be written as

$$u_r=-\frac{1}{r}\frac{\partial\psi}{\partial\theta}\bigg|_{r=D/2}, \qquad u_\theta=\frac{\partial\psi}{\partial r}\bigg|_{r=D/2} \tag{23}$$

which gives

$$u_r=0, \qquad u_\theta=U_\infty f(\theta) \tag{24}$$

where

$$\begin{aligned} f(\theta)=&\sin\theta \\ &-\left(\frac{2\pi C}{S_T}\right)\left[\frac{\cos(\pi D\cos\theta/S_T)\sin\theta}{\cosh(\pi D\cos\theta/S_T)-\cos(\pi D\sin\theta/S_T)}\right. \\ &+\sin\left(\frac{\pi D\sin\theta}{S_T}\right) \\ &\left.\times\frac{\sinh(\pi D\cos\theta/S_T)\cos\theta+\sin\theta\sin(\pi D\sin\theta/S_T)}{[\cosh(\pi D\cos\theta/S_T)-\cos(\pi D\sin\theta/S_T)]^2}\right] \end{aligned} \tag{25}$$

Setting $C_1=\pi D/S_T$ and substituting the value of C, we get

$$\begin{aligned} f(\theta)=&\sin\theta-2\sinh^2\left(\frac{C_1}{2}\right)\left[\frac{\cos(C_1\cos\theta)\sin\theta}{\cosh(C_1\cos\theta)-\cos(C_1\sin\theta)}\right. \\ &\left.+\sin(C_1\sin\theta)\times\frac{\sinh(C_1\cos\theta)\cos\theta+\sin\theta\sin(C_1\sin\theta)}{[\cosh(C_1\cos\theta)-\cos(C_1\sin\theta)]^2}\right] \end{aligned} \tag{26}$$

The resultant potential flow velocity is

$$U = U_\infty f(\theta) \tag{27}$$

Temperature Distribution

Assuming a thin thermal boundary layer around the cylinder, the temperature distribution in the thermal boundary layer can be approximated by a third-order polynomial,

$$(T - T_\infty)/(T_w - T_\infty) = A + B\eta_T + C\eta_T^2 + D\eta_T^3 \tag{28}$$

where $\eta_T = Y/\delta_T(s)$. When the aforementioned thermal boundary conditions are used, the temperature distribution will be

$$(T - T_\infty)/(T_w - T_\infty) = 1 - \tfrac{3}{2}\eta_T + \tfrac{1}{2}\eta_T^3 \tag{29}$$

for the isothermal boundary condition and

$$T - T_\infty = (2q\delta_T/3k_f)\left(1 - \tfrac{3}{2}\eta_T + \tfrac{1}{2}\eta_T^3\right) \tag{30}$$

for the isoflux boundary condition.

Boundary-Layer Parameters

In dimensionless form, the momentum integral equation can be written as

$$\frac{U\delta_2}{\nu}\frac{\mathrm{d}\delta_2}{\mathrm{d}s} + \left(2 + \frac{\delta_1}{\delta_2}\right)\frac{\delta_2^2}{\nu}\frac{\mathrm{d}U}{\mathrm{d}s} = \frac{\delta_2}{U}\frac{\partial u}{\partial Y}\bigg|_{Y=0} \tag{31}$$

where

$$\delta_1 = \delta\int_0^1 \left[1 - \frac{u}{U}\right]\mathrm{d}\eta \tag{32}$$

$$\delta_2 = \delta\int_0^1 \frac{u}{U}\left[1 - \frac{u}{U}\right]\mathrm{d}\eta \tag{33}$$

When velocity distribution from Eq. (15) is used, Eqs. (32) and (33) can be written as

$$\delta_1 = (\delta/10)(3 - \lambda/12) \tag{34}$$

$$\delta_2 = (\delta/63)(37/5 - \lambda/15 - \lambda^2/144) \tag{35}$$

assuming

$$Z = \frac{\delta_2^2}{\nu}, \qquad K = Z\frac{\mathrm{d}U}{\mathrm{d}s}$$

Equation (31) can be reduced to a nonlinear differential equation of the first order for Z, which is given by

$$\frac{\mathrm{d}Z}{\mathrm{d}s} = \frac{H(K)}{U} \tag{36}$$

where $H(K) = 2f_2(K) - 2K[2 + f_1(K)]$ is a universal function and is approximated by Walz[26] using a straight line,

$$H(K) = 0.47 - 6K \tag{37}$$

with

$$f_1(K) = \frac{63(3 - \lambda/12)}{10(37/5 - \lambda/15 - \lambda^2/144)} \tag{38}$$

$$f_2(K) = \frac{1}{63}\left(2 + \frac{\lambda}{6}\right)\left(\frac{37}{5} - \frac{\lambda}{15} - \frac{\lambda^2}{144}\right) \tag{39}$$

$$K = \frac{\lambda}{3963}\left(\frac{37}{5} - \frac{\lambda}{15} - \frac{\lambda^2}{144}\right)^2 \tag{40}$$

When Eq. (36) is solved with Eq. (37), the local dimensionless momentum thickness can be written as

$$\frac{\delta_2}{D} = \frac{0.485}{\sqrt{Re_D}}\sqrt{\frac{1}{f^6(\theta)}\int_0^\theta f^5(\zeta)\,\mathrm{d}\zeta} \tag{41}$$

The local dimensionless boundary-layer thickness can be obtained from Eq. (16),

$$\delta/D = \sqrt{\lambda/2\,Re_D\,g(\theta)} \tag{42}$$

where $g(\theta)$ is the first derivative of $f(\theta)$ with respect to θ obtained from Eq. (26). When Eqs. (35) and (42) are solved and the results are compared with Eq. (41), the values of the pressure gradient parameter λ are obtained corresponding to each position along the cylinder surface. These values are positive from $0 \le \theta \le \theta_1 = \pi/2$, for example, region 1, and negative from $\theta_1 = \pi/2 \le \theta \le \theta_s$, for example, region 2, as shown in Fig. 2. Thus, the whole range of interest $0 \le \theta \le \theta_s$ can be divided into two regions, and the λ values can be fitted separately for each blockage ratio by the least-squares method into two polynomials. These polynomials can be used to determine the drag and the local heat transfer coefficients in both regions.

Fluid Flow

The first parameter of interest is fluid friction, which manifests itself in the form of the drag force F_D, where F_D is the sum of the skin-friction drag D_f and pressure drag D_p. Skin-friction drag is due to viscous shear forces produced at the cylinder surface predominantely in those regions where the boundary layer is attached. The component of shear force in the flow direction is given by

$$D_f = \int_A \tau_w \frac{D}{2}\sin\theta\,\mathrm{d}\theta \tag{43}$$

where τ_w is the shear stress along the cylinder wall, which can be determined from Newton's law of viscosity,

$$\tau_w = \mu\frac{\partial u}{\partial y}\bigg|_{y=0} \tag{44}$$

In dimensionless form, it can be written as

$$C_f = \tau_w \Big/ \tfrac{1}{2}\rho U_\infty^2 = \tfrac{1}{3}\left[(\lambda + 12)\Big/\sqrt{Re_D}\right] f(\theta)\sqrt{2g(\theta)/\lambda} \tag{45}$$

The angle of separation depends only on the velocity distribution outside the boundary layer. Khan et al.[2] have shown that, for infinite flow conditions, separation is calculated to occur at $\theta_s = 107.71$ deg. From Eq. (45) it can be shown that the angle of separation depends on the blockage ratio. The friction drag coefficient is defined as

$$\begin{aligned} C_{Df} &= \int_0^\pi C_f \sin\theta\,\mathrm{d}\theta \\ &= \int_0^{\theta_s} C_f \sin\theta\,\mathrm{d}\theta + \int_{\theta_s}^\pi C_f \sin\theta\,\mathrm{d}\theta \end{aligned} \tag{46}$$

Because no shear stress acts on the cylinder surface after boundary-layer separation, the second integral will be zero and the friction drag coefficient can be written as

$$\begin{aligned} C_{Df} &= \int_0^{\theta_s} C_f \sin\theta\,\mathrm{d}\theta \\ &= \frac{1}{3\sqrt{Re_D}}\left[\int_0^{\theta_1} (\lambda_1 + 12) f(\theta)\sin\theta\sqrt{\frac{2g(\theta)}{\lambda_1}}\,\mathrm{d}\theta \right. \\ &\quad \left. + \int_{\theta_1}^{\theta_s} (\lambda_2 + 12) f(\theta)\sin\theta\sqrt{\frac{2g(\theta)}{\lambda_2}}\,\mathrm{d}\theta\right] \end{aligned} \tag{47}$$

The drag coefficient C_{Df} is calculated for different blockage ratios and correlated into a single expression:

$$C_{Df} = \frac{[45.72 - 39.9\exp(-0.95b^{3.44})]}{\sqrt{Re_D}} \tag{48}$$

Pressure drag is due to the unbalanced pressures that exist between the relatively high pressures on the upstream surfaces and the lower pressures on the downstream surfaces. The component of pressure force in the flow direction is given by

$$D_p = \int_A p\frac{D}{2}\cos\theta\,\mathrm{d}\theta \tag{49}$$

In dimensionless form, it can be written as

$$C_{Dp} = \int_0^{\pi} C_p\cos\theta\,\mathrm{d}\theta \tag{50}$$

where C_p is the pressure coefficient and is defined as

$$C_p = \Delta p \Big/ \tfrac{1}{2}\rho U_\infty^2 \tag{51}$$

The pressure difference Δp is obtained by integrating Eq. (2) with respect to θ. Then the pressure drag coefficient is calculated, using Eq. (50), for different blockage ratios and correlated into a single expression:

$$C_{Dp} = \{6.1 - 4.95\exp(-0.76b^{2.63})\} + \left[\frac{1.49 - 0.23\exp(-5.81b^{2.15})}{Re_D}\right] \tag{52}$$

The total drag coefficient C_D can be written as the sum of both drag coefficients:

$$C_D = \frac{[45.72 - 39.9\exp(-0.95b^{3.44})]}{\sqrt{Re_D}} + [6.1 - 4.95\exp(-0.76b^{2.63})] + \frac{[1.49 - 0.23\exp(-5.81b^{2.15})]}{Re_D} \tag{53}$$

Heat Transfer

The second parameter of interest in this study is the dimensionless average heat transfer coefficient Nu_D for large Prandtl numbers. This parameter is determined by integrating Eq. (8) from the cylinder surface to the thermal boundary-layer edge. When the presence of a thin thermal boundary layer δ_T along the cylinder surface is assumed, the energy integral equation for the isothermal boundary condition can be written as

$$\frac{\mathrm{d}}{\mathrm{d}s}\int_0^{\delta_T}(T - T_\infty)u\,\mathrm{d}Y = -\alpha\left.\frac{\partial T}{\partial Y}\right|_{Y=0} \tag{54}$$

When velocity and temperature profiles are used, and $\zeta = \delta_T/\delta < 1$ is assumed, Eq. (54) can be simplified to

$$\delta_T\frac{\mathrm{d}}{\mathrm{d}s}[U(s)\delta_T\zeta(\lambda + 12)] = 90\alpha \tag{55}$$

Because $s = (D/2)\theta \Rightarrow \mathrm{d}s = (D/2)\,\mathrm{d}\theta$ and $U(s) = U_\infty f(\theta)$, therefore,

$$\delta_T\frac{\mathrm{d}}{\mathrm{d}\theta}[f(\theta)\delta_T\zeta(\lambda + 12)] = \frac{45D^2}{PrRe_D} \tag{56}$$

This equation can be rewritten separately for the two regions mentioned earlier, that is,

$$\delta_T\frac{\mathrm{d}}{\mathrm{d}\theta}[f(\theta)\delta_T\zeta(\lambda_1 + 12)] = \frac{45D^2}{PrRe_D} \tag{57}$$

for region 1, and

$$\delta_T\frac{\mathrm{d}}{\mathrm{d}\theta}[f(\theta)\delta_T\zeta(\lambda_2 + 12)] = \frac{45D^2}{PrRe_D} \tag{58}$$

for region 2. These two equations can be solved separately in the two regions for the local thermal boundary layer thicknesses,

$$\frac{\delta_{T_1}}{D} = \frac{1}{Re_D^{\frac{1}{2}}Pr^{\frac{1}{3}}}\sqrt[3]{\frac{90f_1(\theta)}{(\lambda_1 + 12)^2 f^2(\theta)}\sqrt{\frac{\lambda_1}{2g(\theta)}}} \tag{59}$$

$$\frac{\delta_{T_2}}{D} = \frac{1}{Re_D^{\frac{1}{2}}Pr^{\frac{1}{3}}}\sqrt[3]{\frac{90f_3(\theta)}{f^2(\theta)}\sqrt{\frac{\lambda_2}{2g(\theta)}}} \tag{60}$$

where functions $f_1(\theta)$ and $f_3(\theta)$ are given by

$$f_1(\theta) = \int_0^{\theta} f(\theta)(\lambda_1 + 12)\,\mathrm{d}\theta \tag{61}$$

$$f_2(\theta) = \int_{\theta_1}^{\theta} f(\theta)(\lambda_2 + 12)\,\mathrm{d}\theta \tag{62}$$

$$f_3(\theta) = \frac{f_1(\theta)}{\lambda_1 + 12} + \frac{f_2(\theta)}{\lambda_2 + 12} \tag{63}$$

For the isothermal boundary condition, the local heat transfer coefficient is defined as follows:

$$h(\theta) = -\frac{k_f(\partial T/\partial Y)|_{Y=0}}{T_w - T_\infty} = \frac{3k_f}{2\delta_T} \tag{64}$$

Thus, local heat transfer coefficients for both regions are written as

$$h_1(\theta) = 3k_f\big/2\delta_{T_1}, \qquad h_2(\theta) = 3k_f\big/2\delta_{T_2} \tag{65}$$

which give the local Nusselt numbers for isothermal boundary condition:

$$Nu_{D1}(\theta) = \frac{3}{2}\sqrt[3]{\frac{(\lambda_1 + 12)^2 f^2(\theta)}{90f_1(\theta)}\sqrt{\frac{2g(\theta)}{\lambda_1}}}\,Re_D^{\frac{1}{2}}Pr^{\frac{1}{3}} \tag{66}$$

$$Nu_{D2}(\theta) = \frac{3}{2}\sqrt[3]{\frac{f^2(\theta)}{90f_3(\theta)}\sqrt{\frac{2g(\theta)}{\lambda_2}}}\,Re_D^{\frac{1}{2}}Pr^{\frac{1}{3}} \tag{67}$$

The average heat transfer coefficient is defined as

$$\bar{h} = \frac{1}{\pi}\int_0^{\pi} h(\theta)\,\mathrm{d}\theta = \frac{1}{\pi}\left[\int_0^{\theta_s} h(\theta)\,\mathrm{d}\theta + \int_{\theta_s}^{\pi} h(\theta)\,\mathrm{d}\theta\right] \tag{68}$$

It has been observed experimentally by many researchers that, at low Reynolds numbers (up to $Re_D = 5000$, according to Žukauskas and Žiugžda[9]), there is no appreciable increase in the local heat transfer after the separation point. However, at high Reynolds numbers, the local heat transfer increases from the separation point to the rear stagnation point. Hence, the average heat transfer coefficient can be written as

$$\bar{h} = \frac{1}{\pi}\int_0^{\theta_s} h(\theta)\,\mathrm{d}\theta = \frac{1}{\pi}\left[\int_0^{\theta_1} h_1(\theta)\,\mathrm{d}\theta + \int_{\theta_1}^{\theta_s} h_2(\theta)\,\mathrm{d}\theta\right] \tag{69}$$

When Eqs. (59–65) are used, Eq. (69) can be solved for the average heat transfer coefficient that gives the average Nusselt number for an isothermal cylinder:

$$Nu_D|_{\text{isothermal}} = [0.843 - 0.25\exp(-2.65b^{2.5})]\, Re_D^{\frac{1}{2}} Pr^{\frac{1}{3}} \quad (70)$$

For the isoflux boundary condition, the energy integral equation can be written as

$$\frac{\mathrm{d}}{\mathrm{d}s}\int_0^{\delta_T} (T - T_\infty) u \,\mathrm{d}Y = \frac{q}{\rho c_p} \quad (71)$$

For constant heat flux and thermophysical properties, Eq. (71) can be simplified to

$$\frac{\mathrm{d}}{\mathrm{d}\theta}\left[f(\theta)\delta_T^2 \zeta(\lambda + 12)\right] = \frac{45D^2}{Pr\, Re_D} \quad (72)$$

Rewriting Eq. (72) for the two regions in the same way as Eq. (56), one obtains the dimensionless local thermal boundary layer thicknesses δ_{T_1}/D and δ_{T_2}/D under isoflux boundary condition,

$$\frac{\delta_{T_1}}{D} = \frac{1}{Re_D^{\frac{1}{2}} Pr^{\frac{1}{3}}} \sqrt[3]{\frac{45\theta}{(\lambda_1 + 12) f(\theta)} \sqrt{\frac{\lambda_1}{2g(\theta)}}} \quad (73)$$

$$\frac{\delta_{T_2}}{D} = \frac{1}{Re_D^{\frac{1}{2}} Pr^{\frac{1}{3}}} \sqrt[3]{\frac{45 f_4(\theta)}{f(\theta)} \sqrt{\frac{\lambda_2}{2g(\theta)}}} \quad (74)$$

with

$$f_4(\theta) = \theta/(\lambda_1 + 12) + (\theta - \pi/2)/(\lambda_2 + 12) \quad (75)$$

The local surface temperatures for the two regions is obtained from Eq. (30),

$$\Delta T_1(\theta) = 2q\delta_{T_1}\big/3k_f \quad (76)$$

$$\Delta T_2(\theta) = 2q\delta_{T_2}\big/3k_f \quad (77)$$

The local heat transfer coefficient is obtained from its definition as

$$h_1(\theta) = q/\Delta T_1(\theta), \qquad h_2(\theta) = q/\Delta T_2(\theta) \quad (78)$$

which will give local Nusselt numbers for isoflux boundary condition as follows:

$$Nu_{D1}(\theta) = \frac{3}{2}\sqrt[3]{\frac{(\lambda_1 + 12) f(\theta)}{45\theta} \sqrt{\frac{2g(\theta)}{\lambda_1}}} Re_D^{\frac{1}{2}} Pr^{\frac{1}{3}} \quad (79)$$

$$Nu_{D2}(\theta) = \frac{3}{2}\sqrt[3]{\frac{f(\theta)}{45 f_4(\theta)} \sqrt{\frac{2g(\theta)}{\lambda_2}}} Re_D^{\frac{1}{2}} Pr^{\frac{1}{3}} \quad (80)$$

Following the same procedure for the average heat transfer coefficient as described earlier, one obtains the average Nusselt number for an isoflux cylinder as

$$Nu_D|_{\text{isoflux}} = [1.104 - 0.47\exp(-1.54b^{2.77})] Re_D^{\frac{1}{2}} Pr^{\frac{1}{3}} \quad (81)$$

Combining the results for both thermal boundary conditions, we have

$$\frac{Nu_D}{Re_D^{\frac{1}{2}} Pr^{\frac{1}{3}}} = \begin{cases} 0.843 - 0.25\exp(-2.65b^{2.5}) & \text{for UWT} \\ 1.104 - 0.47\exp(-1.54b^{2.77}) & \text{for UWF} \end{cases} \quad (82)$$

Results and Discussion

Flow Characteristics

The effects of the blockage ratio b on the velocity distribution outside the boundary layer are shown in Fig. 4. It shows that as the blockage ratio decreases the velocity outside the boundary layer decreases. These results are compared with the experimental data of Akilba'yev et al.[19] (reported by Žukauskas[1]) for two blockage ratios. A good agreement between potential theory and experiment is observed for the front part of the cylinder where laminar boundary layer exists.

The dimensionless local shear stress, $C_f\sqrt{(Re_D)}$, is plotted in Fig. 5 for $b = 2.5$. It shows that C_f is zero at the stagnation point and reaches a maximum at $\theta \approx 60$ deg. The increase in shear stress is caused by the deformation of the velocity profiles in the boundary layer, a higher velocity gradient at the wall, and a thicker boundary layer. In the region of decreasing C_f preceding the separation point, the pressure gradient decreases further and finally C_f falls to zero, where boundary-layer separation occurs. Beyond this point, C_f remains close to zero up to the rear stagnation point. These results are compared with the numerical results of Vaitiekünas et al.[21] for the same blockage ratio. The results are again in good agreement for the front part of the cylinder. In Fig. 6, it can be seen that the angle of separation depends on the blockage ratio. As the blockage ratio increases, the location of the boundary-layer separation moves backward. This movement is due to the change in the velocity distribution outside the boundary layer. In Fig. 7, the effects of blockage ratio on the drag coefficient can be seen for different Reynolds numbers. It is clear that the drag coefficient decreases with the blockage

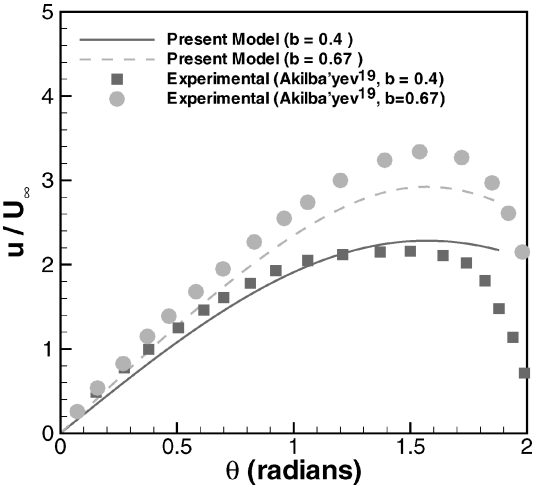

Fig. 4 Effect of blockage ratio on velocity distribution.

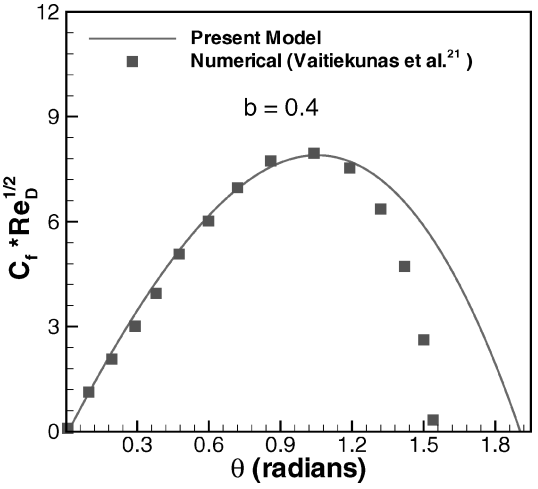

Fig. 5 Distribution of dimensionless shear stress for given blockage ratio.

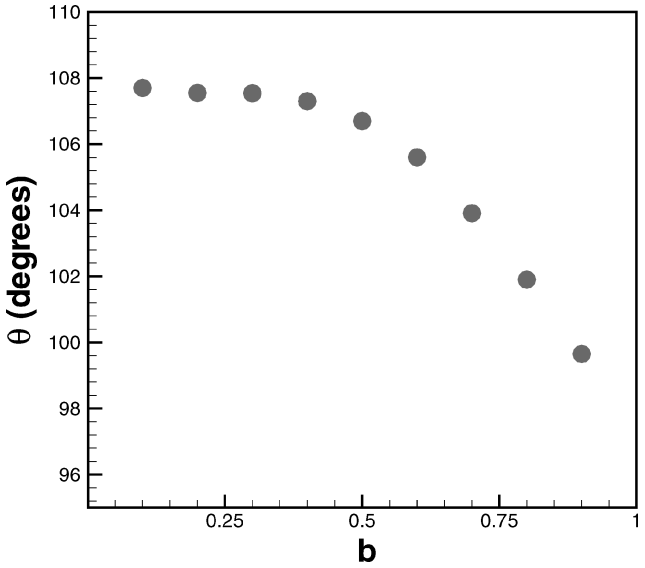

Fig. 6 Effect of blockage ratio on angle of separation.

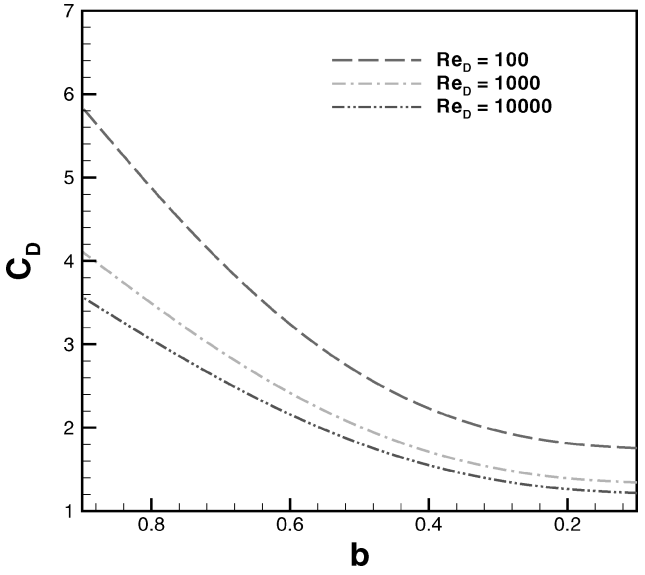

Fig. 7 Effect of blockage ratio and Reynolds number on drag coefficient.

ratio. The variation of the drag coefficient C_D with Reynolds number Re_D for different blockage ratios is shown in Fig. 8. In this case, the drag coefficient decreases with the increase in Reynolds number Re_D for a specific blockage ratio. The present results are compared with the experimental results of Wieselsberger[6] for infinite flow conditions. They are in good agreement except at $Re_D = 2 \times 10^3$, where a downward deviation (23.75%) in the experimental results was noticed. No physical explanation could be found in the literature for this deviation.

Heat Transfer Characteristics

The comparison of local Nusselt numbers for the isothermal and isoflux boundary conditions for a given blockage ratio is shown in Fig. 9. The isoflux boundary condition gives a higher heat transfer coefficient over the larger part of the circumference. On the front part of the cylinder (up to $\theta \approx 40$ deg), there is no appreciable effect of boundary condition. Higher heat transfer coefficients have also been observed experimentally by Perkins and Leppert[18] for a blockage ratio of 0.41 with the isoflux boundary condition.

The results for average heat transfer from a single isoflux cylinder are shown in Fig. 10 for a given blockage ratio and Prandtl number, where they are compared with the experimental and numerical data

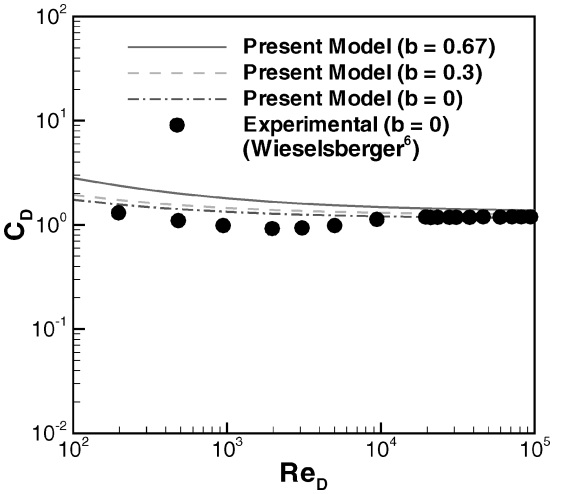

Fig. 8 Drag coefficient as a function of Reynolds number Re_D for different blockage ratios.

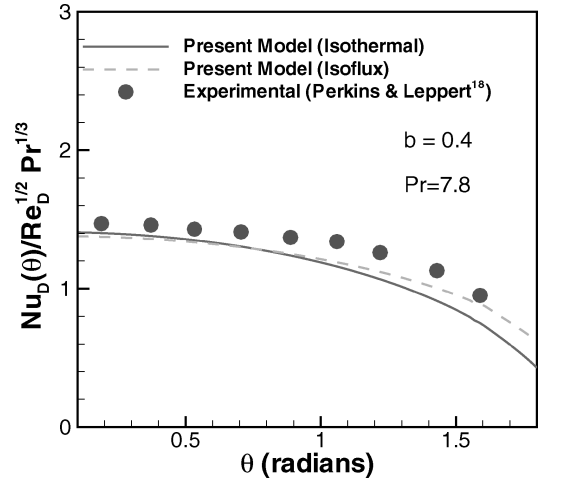

Fig. 9 Local Nusselt number for two thermal boundary conditions.

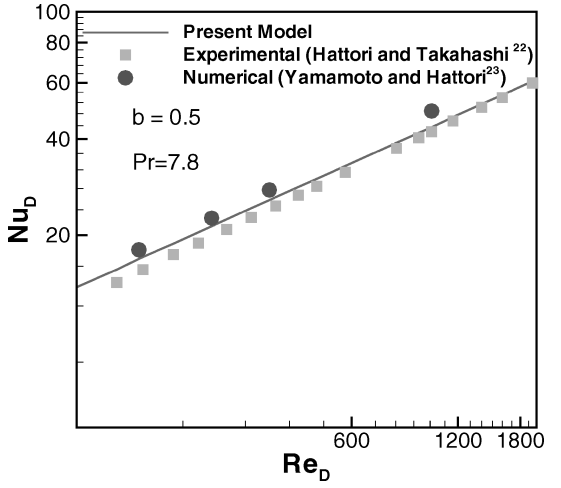

Fig. 10 Average Nusselt number for isoflux cylinder.

of Hattori and Takahashi[22] and Yamamoto and Hattori.[23] It is clear that the present results are in very good agreement with the previous work for a given range of Reynolds numbers.

It is clear from Fig. 11 that the heat transfer values are higher for the smaller blockage ratios, they decrease as the blockage ratio decreases, and finally they approach to the values for an infinite cylinder. The heat transfer values increase with the Reynolds number. The effects of the blockage ratios on the heat transfer

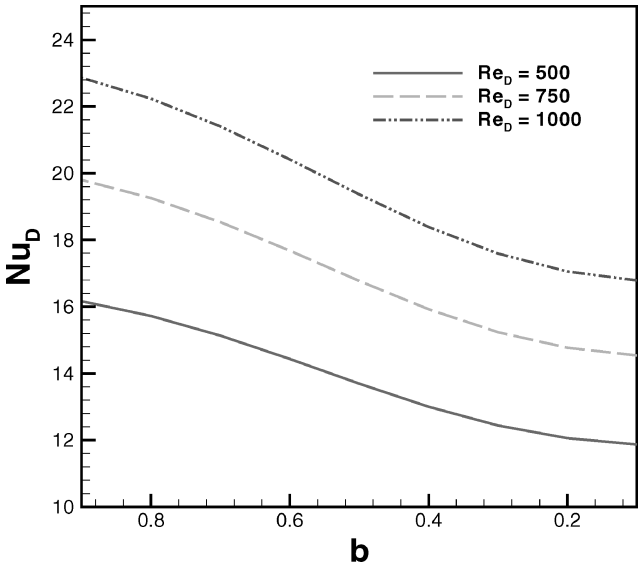

Fig. 11 Effect of blockage ratio and Reynolds number on average Nusselt numbers.

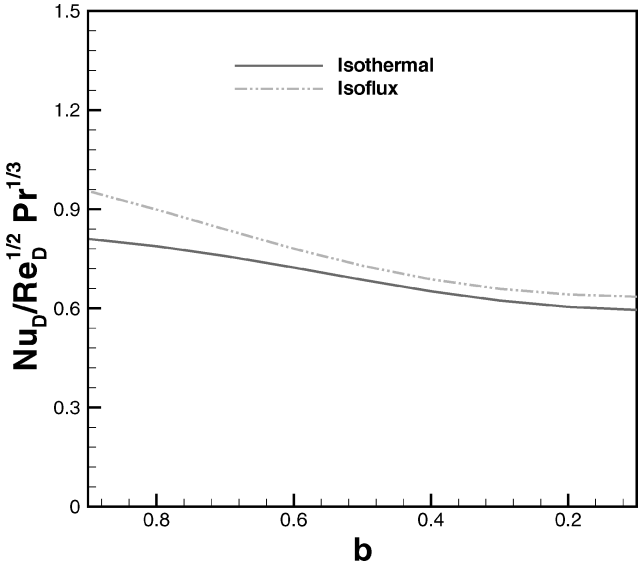

Fig. 12 Effect of blockage ratio and thermal boundary condition on heat transfer.

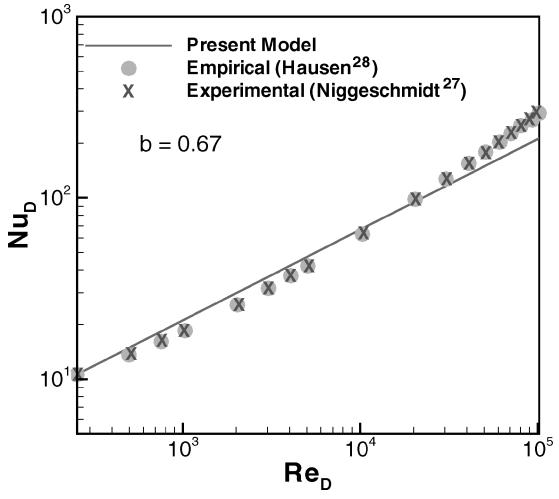

Fig. 13 Average Nusselt number for isothermal boundary condition.

parameter $Nu_D/Re_D^{1/2}Pr^{1/3}$ for the two thermal boundary conditions are shown in Fig. 12. Figure 12 shows that the heat transfer rates are higher for the isoflux boundary condition. Heat transfer rates, for both thermal boundary conditions, decrease first with the blockage ratio and then become constant.

The average Nusselt numbers for the isothermal cylinder for a given blockage ratio are compared in Fig. 13 with the experimental results of Niggeschmidt[27] (reported by Hausen[28]) and Hausen.[28] The average Nusselt number Nu_D values are found to be in a good agreement with both results. However, both previous results are found to be higher at high Reynolds number due to freestream turbulence.

Summary

The influence of blockage ratio on the fluid flow and heat transfer from a circular cylinder, placed between two parallel planes, has been investigated. The method of images is used to obtain the velocity distribution outside the boundary layer. Three correlations are obtained, Eq. (53) for total drag coefficient, Eq. (70) for heat transfer from an isothermal cylinder, and Eq. (81) for heat transfer from a cylinder under the isoflux boundary condition. These correlations can be used to determine the drag coefficient and the dimensionless heat transfer coefficient from a cylinder confined in a channel with different blockage ratios. The present results indicate good agreement with the experimental/numerical results for a wide range of blockage ratio, Reynolds numbers, and Prandtl numbers.

Acknowledgments

The authors gratefully acknowledge the financial support of Natural Sciences and Engineering Research Council of Canada and the Centre for Microelectronics Assembly and Packaging.

References

[1]Žukauskas, A., *Advances in Heat Transfer*, Academic Press, New York, 1972, pp. 93–160.

[2]Khan, W. A., Culham, J. R., and Yovanovich, M. M., "Fluid Flow and Heat Transfer from a Pin-Fin: Analytical Approach," AIAA Paper 2003-163, Jan. 2003.

[3]Roshko, A., "Experiments on the Flow Past Circular Cylinders at Very High Reynolds Number," *Journal of Fluid Mechanics*, Vol. 10, No. 3, 1961, pp. 345–356.

[4]Achenbach, E., "Total and Local Heat Transfer From a Smooth Circular Cylinder in Cross Flow at High Reynolds Number," *International Journal of Heat and Mass Transfer*, Vol. 18, No. 12, 1975, pp. 1387–1396.

[5]Schlichting, H., *Boundary Layer Theory*, 7th ed., McGraw–Hill, New York, 1979, Chap. 10.

[6]Wieselsberger, C., "New Data on The Laws of Fluid Resistance," NACA TN 84, March 1922.

[7]Churchill, S. W., *Viscous Flows: The Practical Use of Theory*, Butterworths Ser. in Chemical Engineering, Butterworths, Boston, 1988, pp. 317–358.

[8]Sucker, D., and Brauer, H., "Investigation of the Flow Around Transverse Cylinders," *Wärme- und Stoffübertragung*, Vol. 8, No. 3, 1975, pp. 149–158.

[9]Žukauskas, A., and Žiugžda, J., *Heat Transfer of a Cylinder in Crossflow*, Hemisphere, New York, 1985.

[10]Eckert, E. R. G., and Soehngen, E., "Distribution of Heat-Transfer Coefficients Around Circular Cylinders in Cross Flow at Reynolds Numbers from 20 to 500," *Transactions of the ASME*, Vol. 74, April 1952, pp. 343–347.

[11]Churchill, S. W., and Bernstein, M., "A Correlating Equation for Forced Convection from Gases and Liquids to a Circular Cylinder in Cross Flow," *Journal of Heat Transfer*, Vol. 99, No. 2, 1977, pp. 300–306.

[12]Morgan, V. T., "The Overall Convective Heat Transfer from Smooth Circular Cylinders," *Advances in Heat Transfer*, Vol. 11, Academic Press, New York, 1975, pp. 199–264.

[13]Hilpert, R., "Wärmeabgabe von geheizten Drahten und Rohren," *Forsch. Geb. Ingenieurwes*, Vol. 4, 1933, pp. 215–224.

[14]Refai-Ahmed, G., and Yovanovich, M. M., "Analytical Method for Forced Convection from Flat Plates, Circular Cylinders, and Spheres," *Journal of Thermophysics and Heat Transfer*, Vol. 9, No. 3, 1995, pp. 516–523.

[15]Krall, K. M., and Eckert, E. R. G., "Heat Transfer to a Transverse Circular Cylinder at Low Reynolds Number Including Refraction Effects," *Heat Transfer*, Vol. 3, 1970, pp. 225–232.

[16]Giedt, W. H., "Investigation of Variation of Point Unit Heat-Transfer Coefficient Around a Cylinder Normal to an Air Stream," *Transactions of the ASME*, Vol. 71, May 1949, pp. 375–381.

[17]Sarma, T. S., and Sukhatme, S. P., "Local Heat Transfer from a Horizontal Cylinder to Air in Cross Flow: Influence of Free Convection and Free Stream Turbulence," *International Journal of Heat and Mass Transfer*, Vol. 20, No. 1, 1977, pp. 51–56.

[18]Perkins, H. C., and Leppert, G., "Local Heat Transfer Coefficients on a Uniformly Heated Cylinder," *International Journal of Heat and Mass Transfer*, Vol. 7, No. 2, 1964, pp. 143–158.

[19]Akilba'yev, Z. S., Isata'yev, S. I., Krashtalev, P. A., and Masle'yeva, N. V., "The Effect of Channel Blockage on the Local Heat Transfer Coefficient of a Uniformly Heated Cylinder," *Problemy Teploenergetyki i Prikladnoi Teplofiziki*, Vol. 3, 1966, pp. 179–198.

[20]Merk, H. J., "Rapid Calculations for Boundary Layer Transfer Using Wedge Solutions and Asymptotic Expansions," *Journal of Fluid Mechanics*, Vol. 5, 1959, pp. 460–480.

[21]Vaitiekünas, P. P., Bulota, A. J., and J. J., "Analysis of the Effect of Duct Blocking on Crossflow and Heat Transfer of a Cylinder," *Heat Transfer—Soviet Research*, Vol. 17, No. 4, 1985, pp. 79–86.

[22]Hattori, N., and Takahashi, T., "Heat Transfer from a Single Row of Circular Cylinders Placed in the Transverse Direction of Water Flow," *Transactions of the Japan Society of Mechanical Engineers*, Pt. B, Vol. 59, No. 568, 1993, pp. 4064–4068.

[23]Yamamoto, H., and Hattori, N., "Flow and Heat Transfer Around a Single Row of Circular Cylinders," *Heat Transfer—Japanese Research*, Vol. 25, No. 3, 1996, pp. 192–200.

[24]Pohlhausen, K., "Zur Näherungsweise Integration der Differential Gleichung der Laminaren Reibungschicht," *Zeitschrift für angewandte Mathematic und Mechanic*, Vol. 1, 1921, pp. 252–268.

[25]Kochin, N. E., Kibel, I. A., and Roze, N. V., *Theoretical Hydromechanics* (translated from 5th Russian edition), Interscience, New York, 1964, Chap. 5.

[26]Walz, A., "Ein neuer Ansatz für das Greschwindligkeitsprofil der laminaren Reibungsschicht," *Lilienthal-Bericht*, Vol. 141, 1941, p. 8.

[27]Niggeschmidt, W., "Druckverlust und Warmeubergang bei fluchtenden, versetzten und teilversetzten querangestromten Rohrbundeln," Dissertation, Darmstadt, Germany, 1975.

[28]Hausen, H., *Heat Transfer in Counterflow, Parallel Flow and Cross Flow*, McGraw–Hill, New York, 1983, Chap. 2.